Supporting Information

Highly Efficient Walking Perovskite Solar Cells Based on Thermomechanical Polymer Films

Jiabin Qi[ab], Linpeng Li[a], Hao Xiong[b], Aurelia Chi Wang[c], Chengyi Hou[a], Qinghong Zhang[b*], Yaogang Li[b], Hongzhi Wang[a*]

[a]*State Key Laboratory for Modification of Chemical Fibers and Polymer Materials, Donghua University, Shanghai 201620, People's Republic of China*

[b]*Engineering Research Center of Advanced Glasses Manufacturing Technology, MOE, Donghua University, Shanghai 201620, People's Republic of China*

[c]*School of Materials Science and Engineering, Georgia Institute of Technology, Atlanta, Georgia 30332, USA*

[*] Corresponding author. Tel: +86-21-67792943; fax: +86-21-67792855.
E-mail address: wanghz@dhu.edu.cn (H. Z. Wang), zhangqh@dhu.edu.cn (Q. H. Zhang).

Supporting Figures

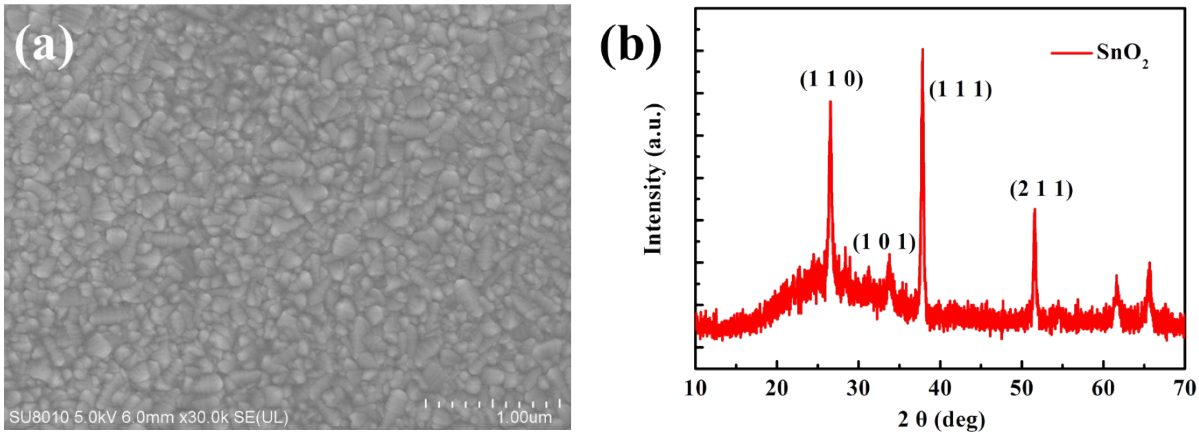

Figure S1. (a) SEM image and (b) XRD patterns of LT-SnO_2.

XRD and SEM were used to analyze the phase composition and microstructure of LT-SnO_2. As shown in **Figure S1**, LT-SnO_2 was uniformly coated on the surface of the ITO/PET substrate to give a constant layer thickness. The LT-SnO_2 layer was bound strongly to the substrate. The XRD pattern of LT-SnO_2 exhibited strong peaks consistent with the (110), (111), and (211) reflections of SnO_2, indicating that the quality of SnO_2 was improved using the hydrothermal method.

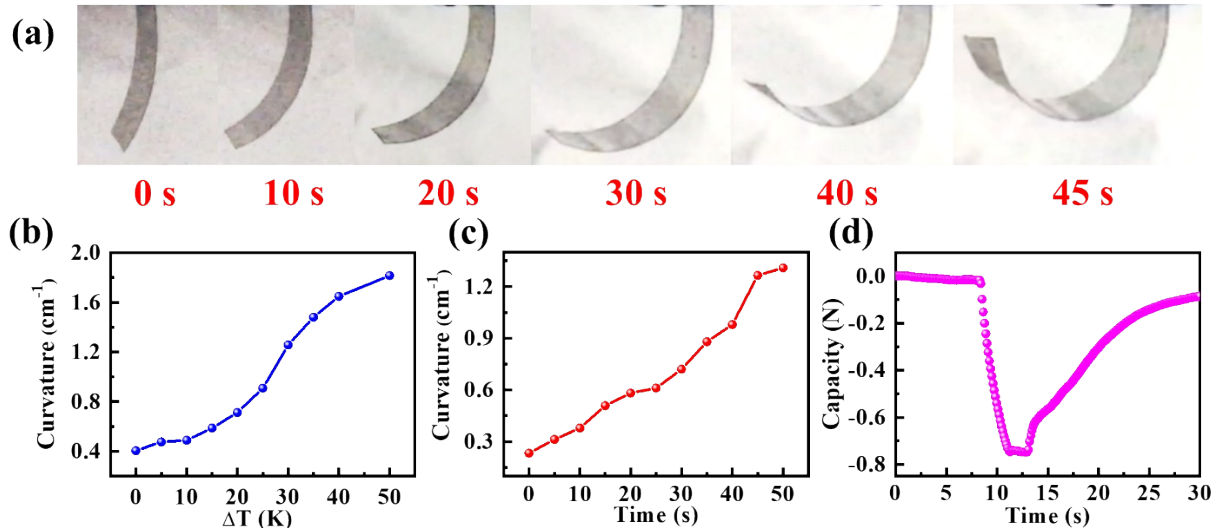

Figure S2. (a) Actuation performance of the film, showing its bending movement at 80 ℃. (b) Curvature of the film as a function of temperature difference. (c) Maximum curvature as a function of time at 80 ℃. (d) Mechanical properties of the actuator.

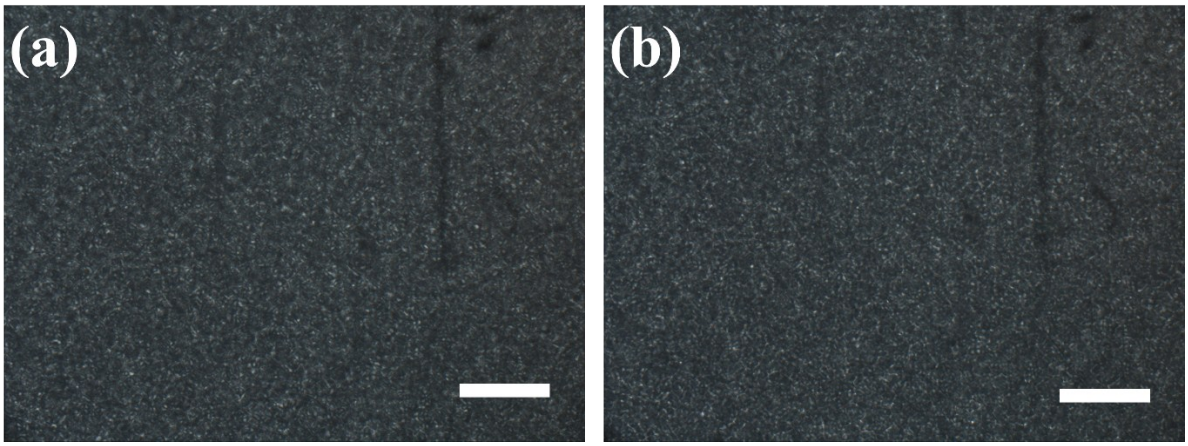

Figure S3. Polarizing optical microscope diagram showing almost no grain size change of PP crystal (scale bar for 200 μm), (a) for 20 ℃ and (b) for 80 ℃.

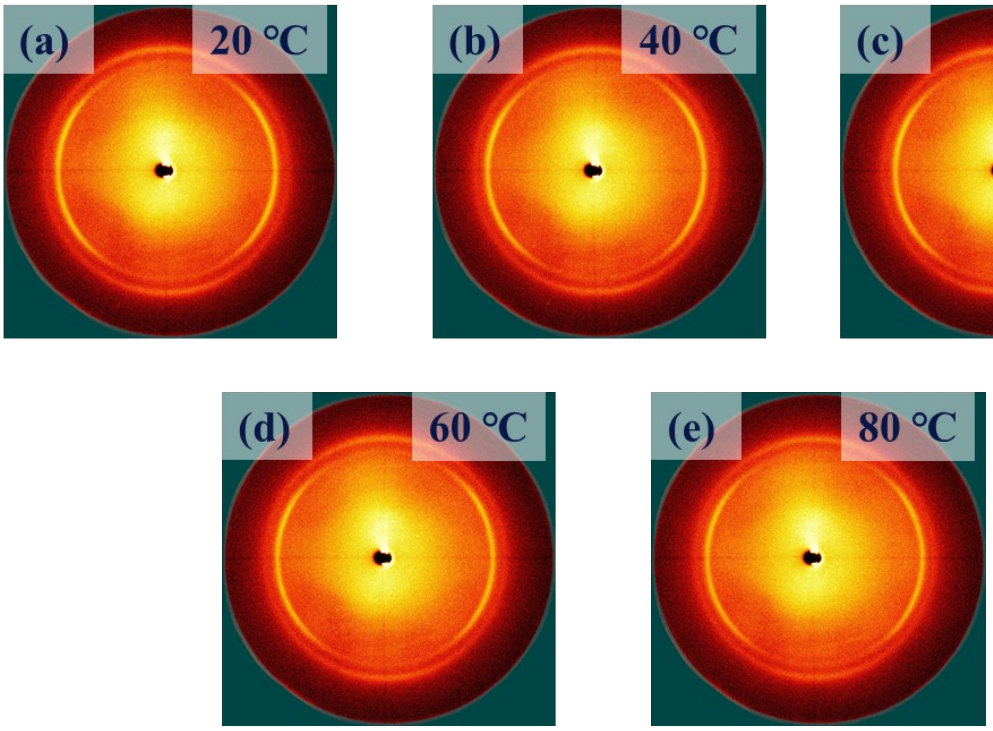

Figure S4. In-situ 2D-XRD images of the LDPE membrane at different temperatures.

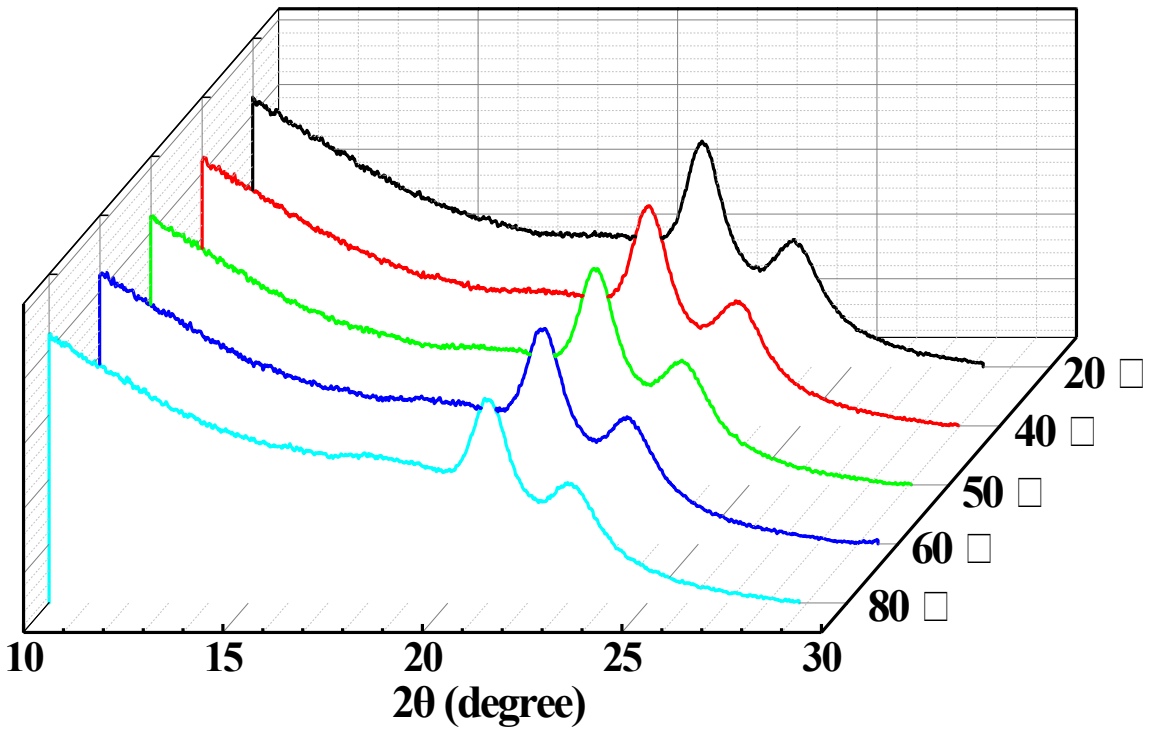

Figure S5. In-situ 2D-XRD patterns of the LDPE membrane at different temperatures.

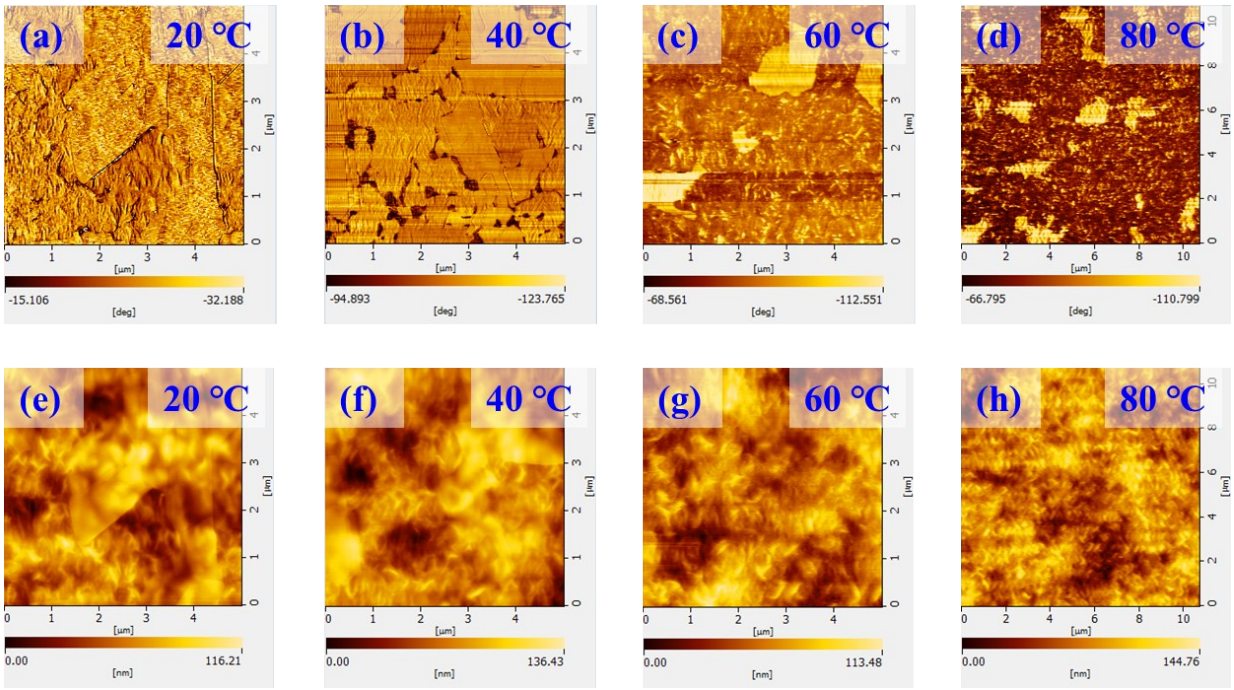

Figure S6. In-situ AFM images of an LDPE film at different temperatures (a–d: phase diagrams; e–h: height images).

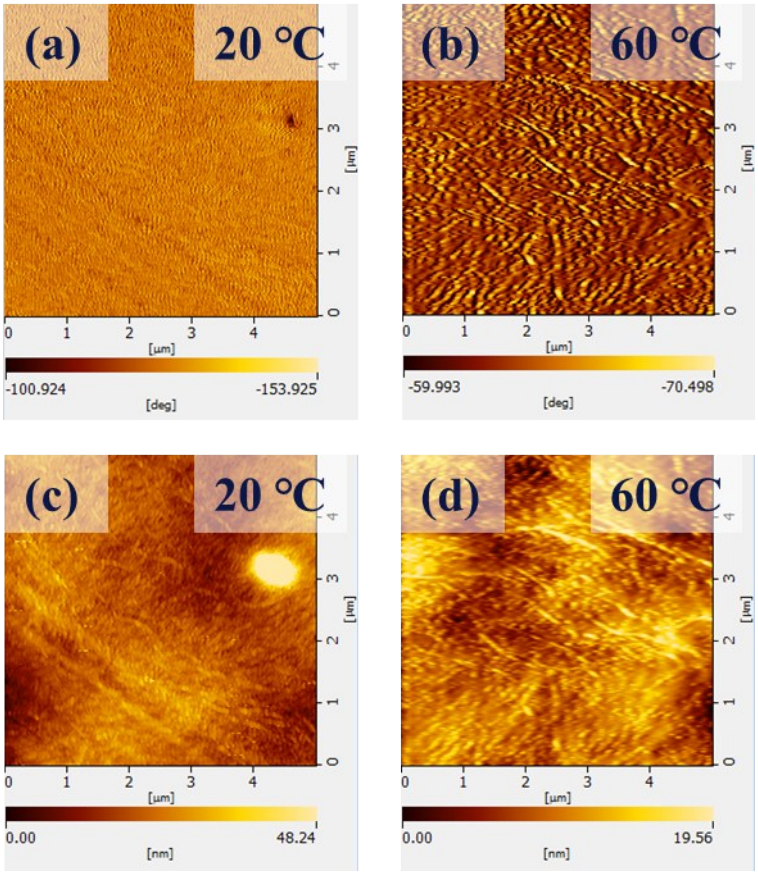

Figure S7. In-situ AFM images of a PP film at different temperatures (a, b: phase diagrams; c, d: height images).

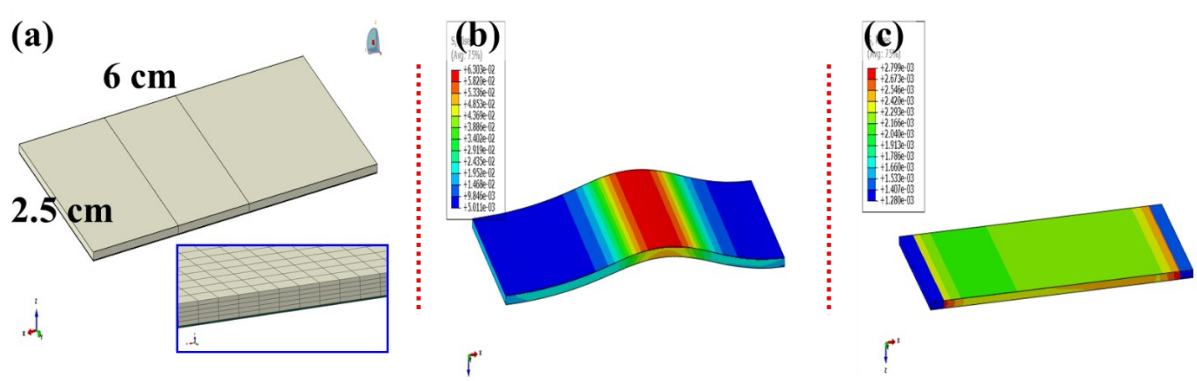

Figure S8. (a) Model of the LDPE/PP actuator. (b) Mises stress cloud image of the LDPE/PP film after light irradiation for 10 s. (c) Residual thermal stress image of the LDPE/PP film after cooling for 40 s.

To decrease the scale of the calculation, it was necessary to simplify the geometry, material properties, and boundary conditions of the model. After debugging, the 2.5 cm edge of the LDPE/PP film was taken as a fixed boundary and the freedom in three directions was constrained. The film edge with a length of 6 cm was considered a symmetrical boundary and its normal freedom was constrained, as shown in **Figure S8a**.

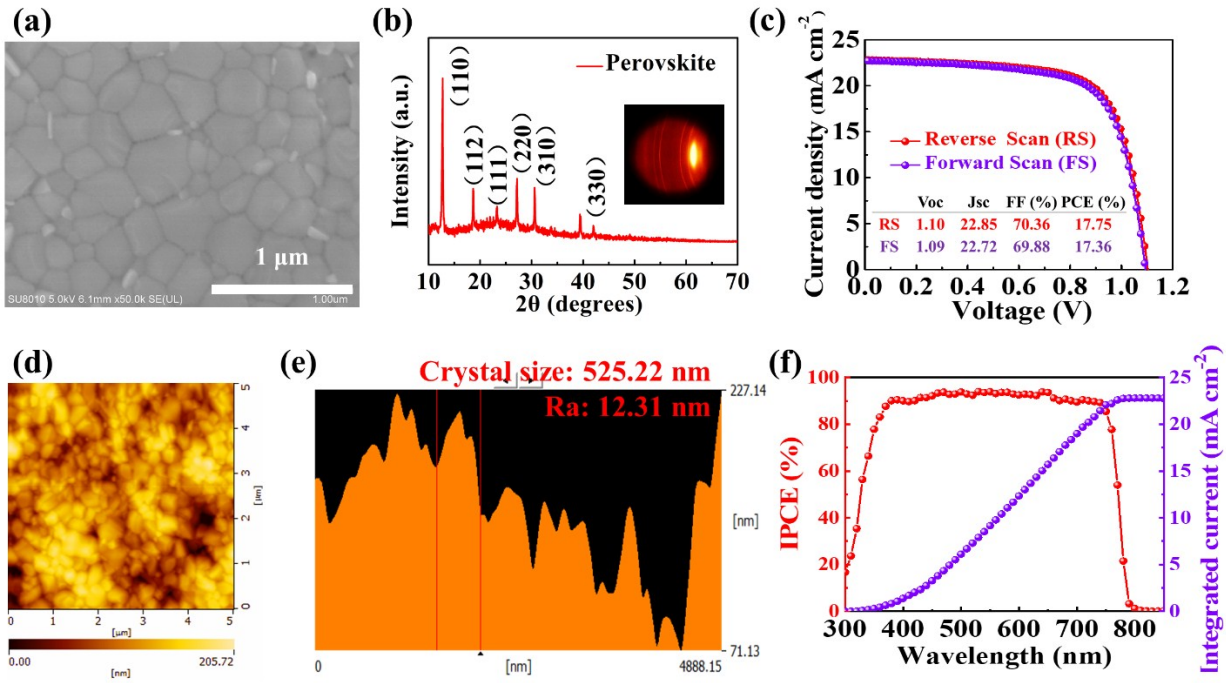

Figure S9. (a) SEM image of the perovskite layer. (b) XRD pattern of the perovskite layer. (c) *J-V* curves of perovskite devices. (d) AFM image and (e) height profile of an ITO-PET/SnO_2/perovskite structure. (f) Incident photon-to-current conversion efficiency (IPCE) of perovskite devices.

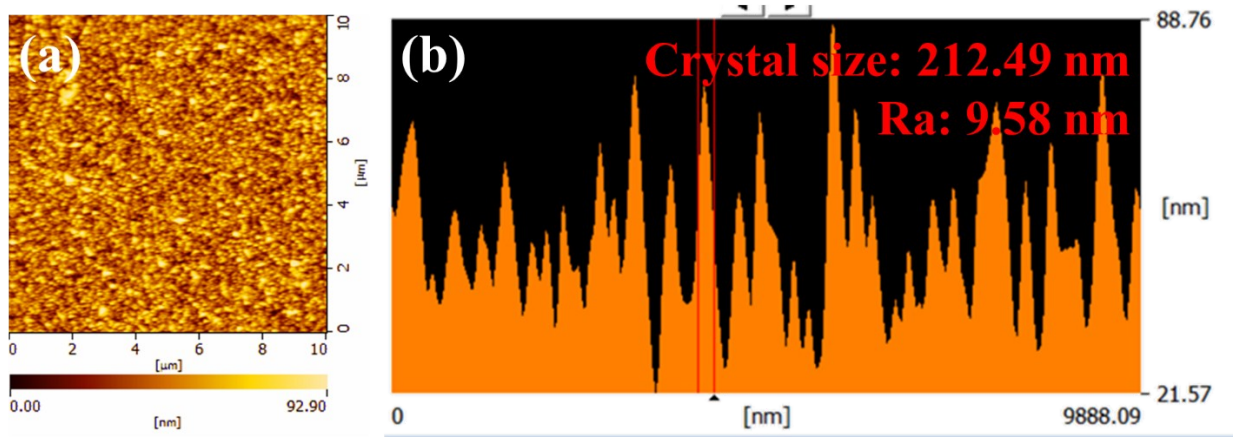

Figure S10. (a) AFM image and (b) height profile of ITO/PET/SnO_2.

Figure S10 presents the surface morphology and average surface roughness (Ra) of the SnO_2 layer. The SnO_2 layer was very smooth with Ra = 9.58 nm, even though the SnO_2 grain size was 200 nm, because the SnO_2 layer was spin coated on an ultrasmooth ITO/PET substrate.

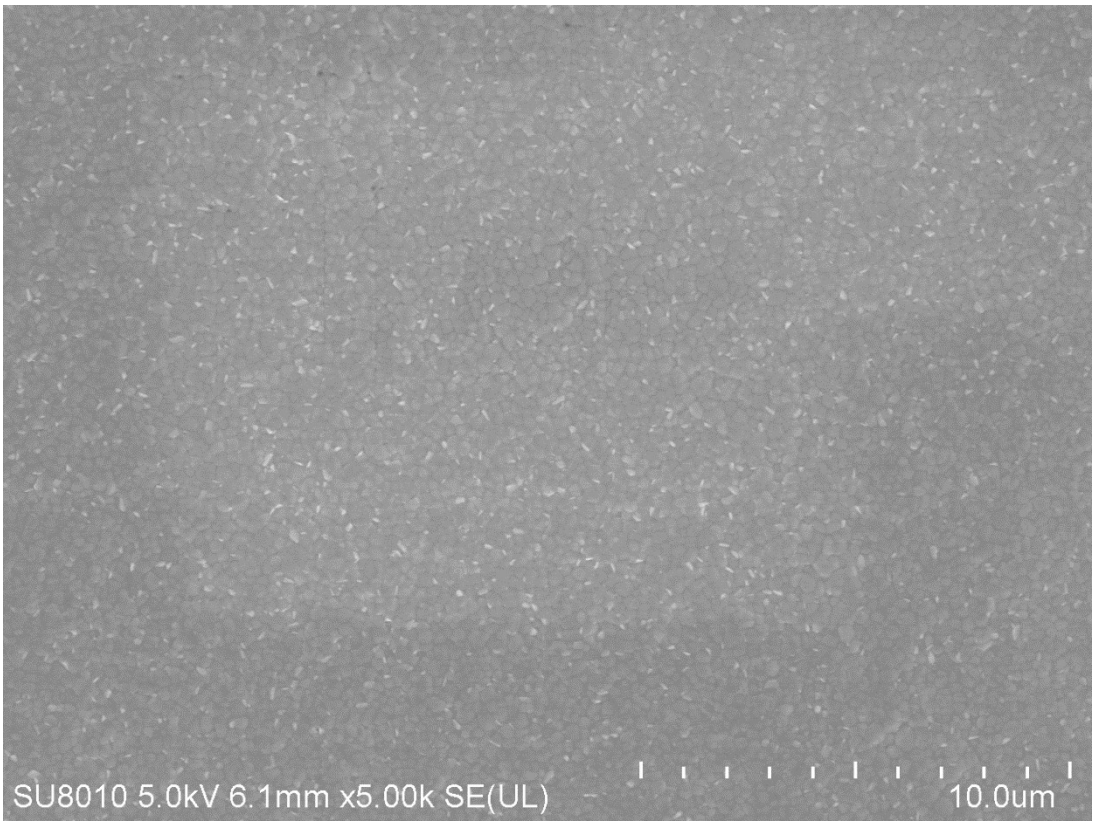

Figure S11. Top-view SEM image of a perovskite film on an LT-SnO_2 layer.

The perovskite film contained large grain sizes of about 500 nm, as determined from Figure S9. The large grains resulted in a low content of grain boundaries, which has been shown to increase the performance of perovskite solar cells. Moreover, the large grain size also indicates the high crystallization of the perovskite film, which was also confirmed by the XRD analysis.

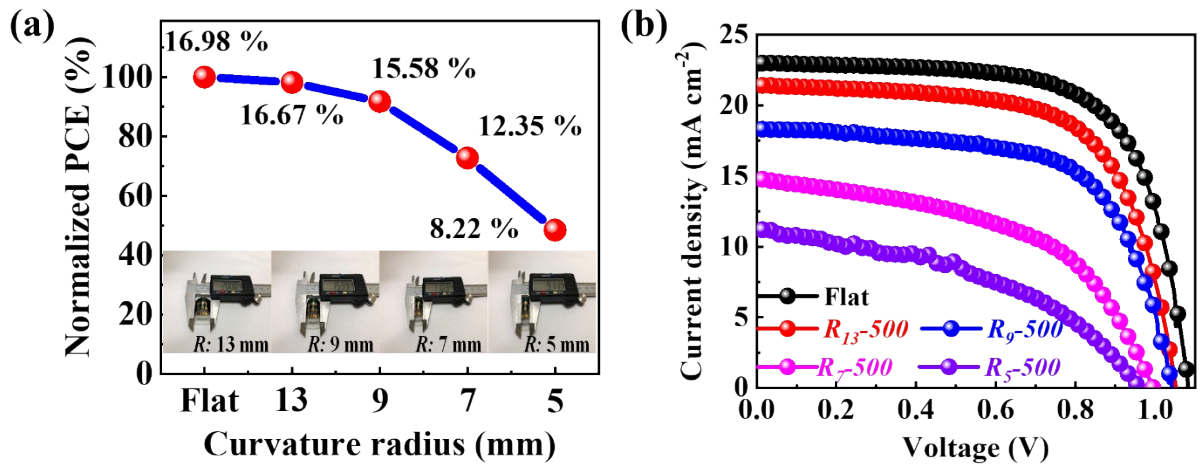

Figure S12. (a) Normalized PCE measured after bending at different curvature radii. (b) *J-V* characteristics of flexible PSCs after 500 repeated bending cycles at different curvature radii.

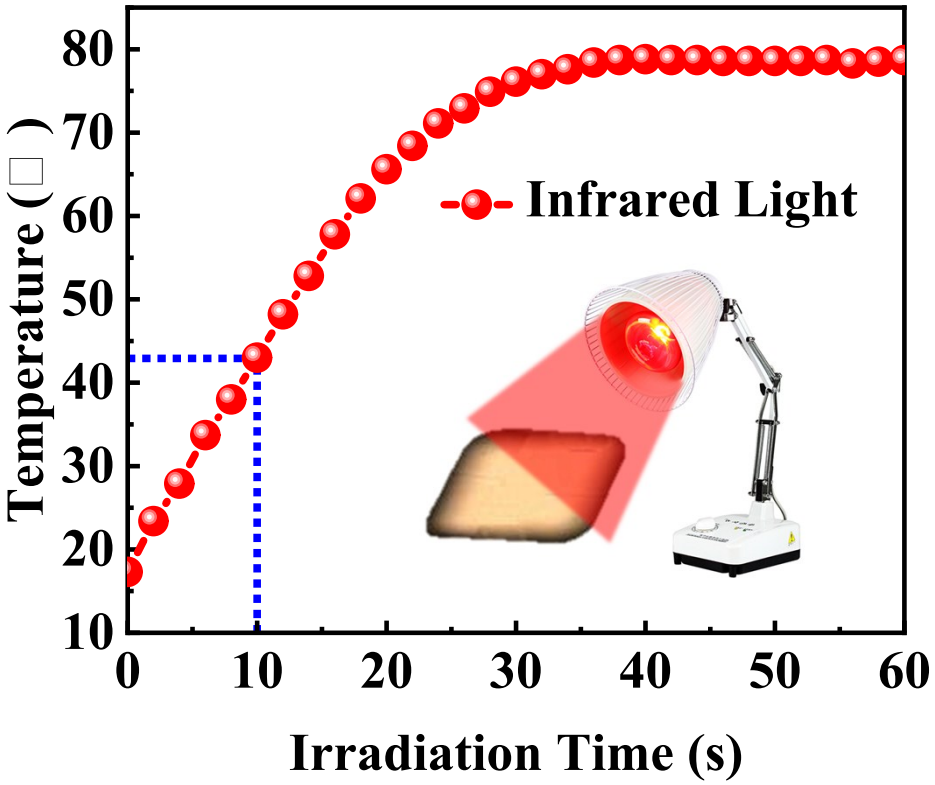

Figure S13. Temperature variation curve of PSCs under NIR light irradiation.

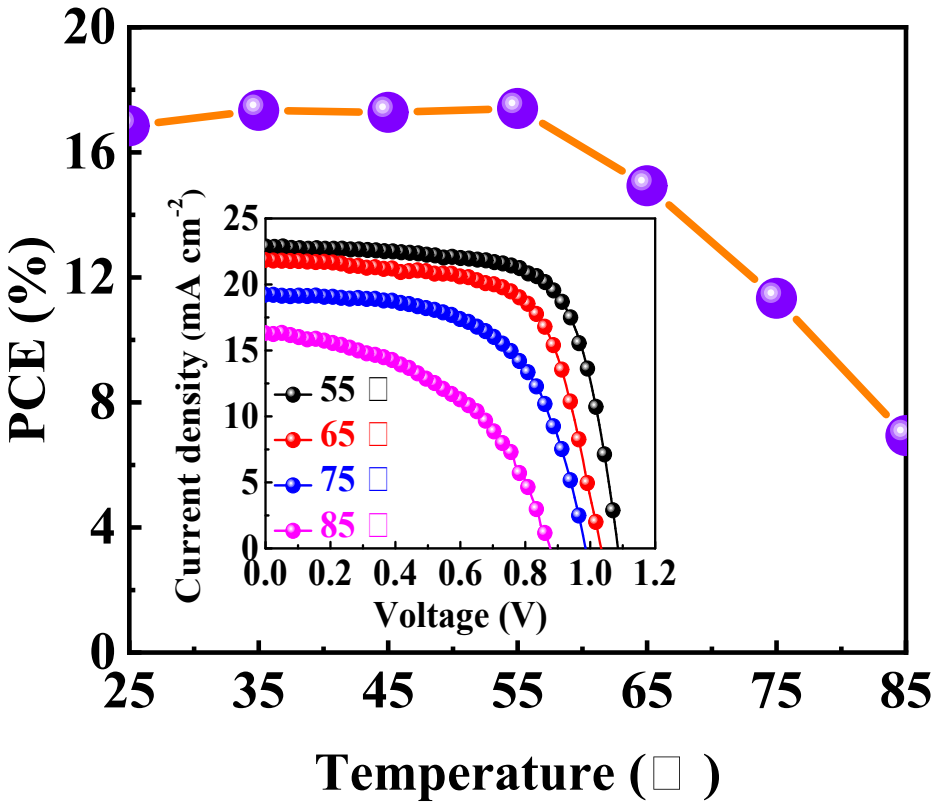

Figure S14. PCE of the PSCs as a function of temperature, inserted graph is *J-V* characteristics of a PSC during temperature changes of 55-85 ℃.

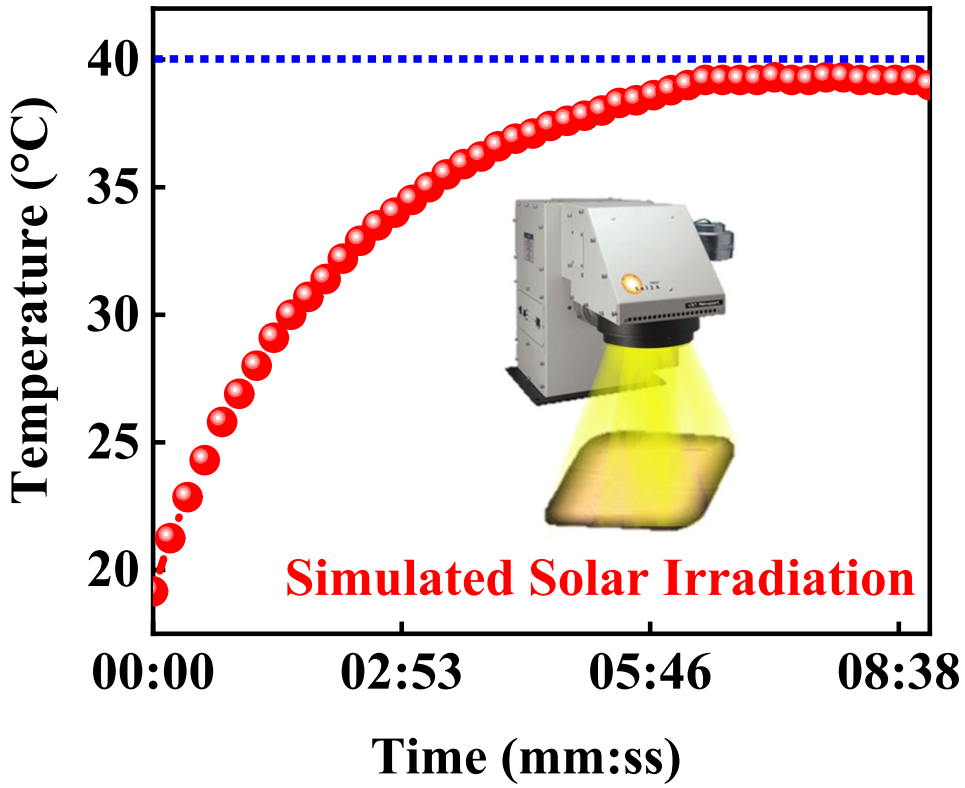

Figure S15. Temperature variation curve of actuating device under simulated solar irradiation.

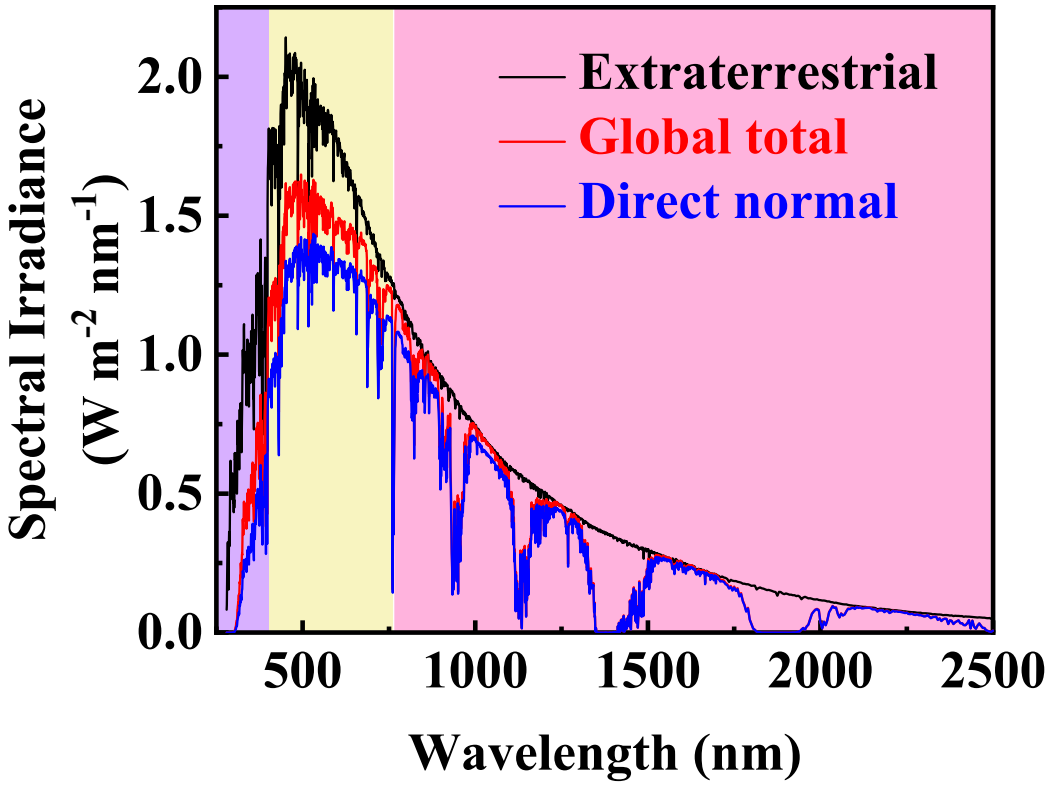

Figure S16. ASTM G173-03 reference spectra. [1]

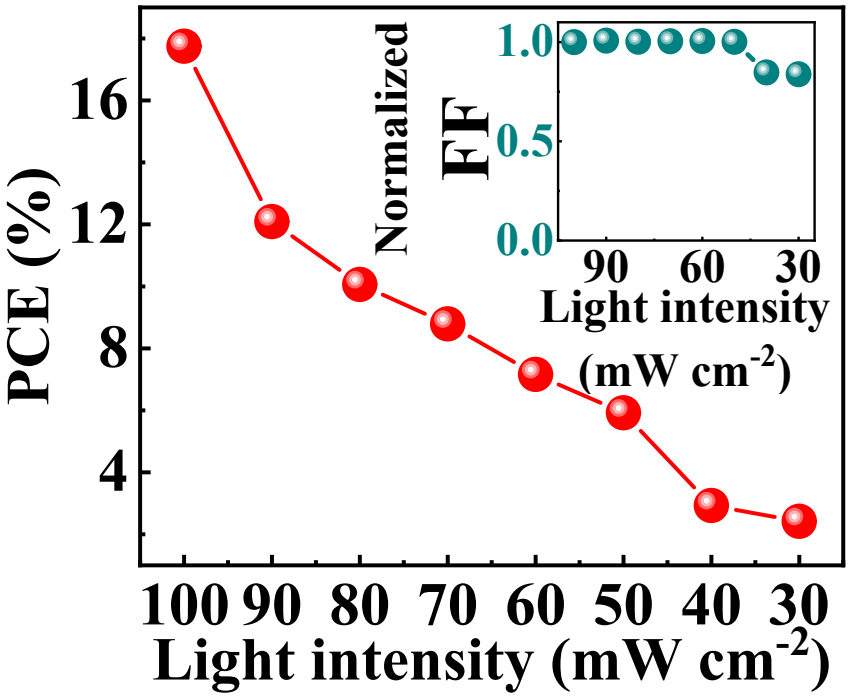

Figure S17. PCE and normalized FF of perovskite solar cells at different light intensities.

Supporting Tables

Table S1. Coefficient of thermal expansion (CTE) values for some common polymers. [2]

Polymer Name	Min Value (10^{-5} / °C)	Max Value (10^{-5} / °C)
PP (Polypropylene)	7	17
PMMA (Poly(methyl methacrylate))	18	25
PS (Polystyrene)	20	29
PVA (Poly(vinyl alcohol))	28	35
PA (Polyamide)	47	66
Natural Rubber	64	66
PE (Poly ethylene)	67	79

Table S2. Parameters of LDPE and PP used in the finite element analysis model.

	LDPE	PP
Density	0.925 g/cm^3	0.900 g/cm^3
Elastic modulus	260 MPa	890 MPa
Poisson ratio (25°C)	0.40	0.42
Specific heat	2.093kj/kg*°C	1.926kj/kg*°C
Thermal conductivity	0.335w/m*°C	0.138w/m*°C
Thermal diffusivity	16 α*10^8 (m^2/s)	8 α*10^8 (m^2/s)

Table S3. Parameters of flexible PSCs measured after bending at different curvature radii.

Bending radius (mm)	Voc (V)	Jsc (mA cm^{-2})	FF (%)	PCE (%)
Flat	1.08	23.00	68.16	16.97
13	1.08	22.91	67.39	16.67
9	1.05	22.58	65.62	15.58
7	1.02	20.28	59.53	12.35
5	0.98	16.37	51.29	8.22

Table S4. Parameters of perovskite solar cells with different incident angles of simulated solar light.

Angle	Voc (V)	Jsc (mA cm^{-2})	FF (%)	PCE (%)
90°	1.10	22.85	70.36	17.75
	1.07	22.67	70.76	17.20
Large Angle	1.07	20.29	70.95	15.48
	1.06	19.49	71.23	14.82
↓	1.06	16.09	70.90	12.15
	1.06	13.73	71.48	10.40
Small Angle	1.03	7.66	71.21	5.72
	1.01	4.92	70.25	3.49
0°	0.99	2.34	70.53	1.66

Table S5. Parameters of perovskite solar cells at different light intensities.

Light intensity (mW cm^{-2})	Voc (V)	Jsc (mA cm^{-2})	FF (%)	PCE (%)
100	1.10	22.85	70.36	17.75
90	1.06	16.06	70.86	12.09
80	1.03	13.84	70.47	10.06
70	1.03	12.04	70.65	8.79
60	1.02	9.86	70.73	7.16
50	1.03	8.08	70.45	5.92
40	0.99	4.96	59.61	2.93
30	0.99	4.13	58.98	2.42

References

(1) National Renewable Energy Laboratory, Reference Air Mass 1.5 Spectra; https://www.nrel.gov/grid/solar-resource/spectra-am1.5.html (accessed date: 06-28-2019).

(2) James E. Mark, Physical Properties of Polymers Handbook. **2007**, *Chapter 7*.